富山大学水素同位体科学研究センター研究報告20：43−52，2000.

論文

含水素炭素膜と金属基板 (Be, Mo, W) との反応動力学の解析

芦田　完，波多野雄治，渡辺国昭

富山大学水素同位体科学研究センター

〒 930-8555 富山市五福 3190

Kinetic Analysis of Reactions between Hydrogen-containing Carbon Film and Substrate Metals (Be, Mo, W)

Kan Ashida, Yuhji Hatano and Kuniaki Watanabe

Hydrogen Isotope Res. Centr.,

Toyama Univ., Gofuku 3190, Toyama 930-8555, Japan

(Received February 9, 2001; Accepcted March 15, 2002)

ABSTRACT

Kinetic analyses were performed for solid-state reactions between a hydrogen-containing carbon film and substrate metals to form metallic carbide of Me_2C (Me = Be, Mo, W). Isothermal and non-isothermal reaction curves could be explained by a random nucleation and two-dimensional crystal growth model. The kinetic equation can be approximated well by $-\ln(1-x) = k_{app}\, t^2$, where x is the extent of reaction and k_{app} the apparent rate constant. The temperature dependence of the rate constants are given as

$$\begin{aligned} k_{app}(\mathrm{Be}) &= 3.10 \exp(-109.\,[\mathrm{kJ/mol}]/RT) \quad [1/\mathrm{sec}^2], \\ k_{app}(\mathrm{Mo}) &= 231.\ \exp(-161.\,[\mathrm{kJ/mol}]/RT), \\ k_{app}(\mathrm{W}) &= 516.\ \exp(-183.\,[\mathrm{kJ/mol}]/RT), \end{aligned}$$

for Be-C, Mo-C and W-C systems, respectively, where the apparent activation energy is considered to be the sum of those for nucleation and diffusion. Linear relations were found between the apparent activation energy and the melting point of substrate metals as well as the bond strength of Me-C (Me=Be, Mo, W).

1. Introduction

Low-Z materials such as beryllium, boron and carbon were widely used in tokamaks to improve plasma confinement parameters by reduction of radiation losses[1, 2]. A serious problem has arisen, however, for their use as protective tiles on the inner wall of tokamaks because of their high erosion rates through physical and chemical sputtering, evaporation, etc. On the other hand, high-Z materials such as molybdenum and tungsten have recently attracted great attention to compensate for low-Z materials with their durability against high heat loading and particle fluence[3].

Installation of two or more plasma facing materials is common now in many tokamaks to control plasma surface interactions, but poses a new problem concerning fuel recycling and inventory, which deeply relate with the physiochemical properties of co-existing layers consisting of low- and high-Z materials. An understanding of the properties of co-existing layers is indispensable for material selection on designing next generation tokamaks.

From this viewpoint, the present authors have investigated physico-chemical properties of hydrogen-containing carbon films deposited on Be, Mo and W[4, 5, 6, 7]. It has been observed that vacuum heating of these films gives rise to the formation of corresponding metal carbides of Me_2C form. This indicates that significant change in fuel recycling and inventory should take place in tokamaks using high- and low-Z materials together, owing to the carbide formation as having been observed for graphite with iron impurity[8, 9, 10].

Carbide formation significantly depends on the substrate. Beryllium carbide is easily formed by vacuum heating at 773 K in ten minutes, whereas tungsten requires the heating above 973 K. Simple relations have been observed between the rate of carbide formation and physico-chemical properties of the substrates[7]. On account of these relations, one can predict the reactivity of hydrogen-containing carbon films with substrate metals. However, details of reaction kinetics and mechanisms have been left as open questions. This paper focuses attention on the kinetics and mechanisms of the carbide formation. The understanding of reaction mechanisms is indispensable to quantitative prediction of property changes of carbons depositing on high-Z metals in tokamaks.

2. Experimental

Hydrogen-containing carbon films were prepared on beryllium, molybdenum and tungsten plates by inductive RF discharge of methane and ethylene[11]. Hereafter, they are denoted as C(H)/M (M=Be, Mo, W) in the present paper. The size of each plate was 10 × 10 × 0.5

mm and the thickness of films was around 0.5 μm. The procedures and the device for sample preparation are described elsewhere[5, 6, 11].

The reaction between the deposited carbon film and substrate was measured at elevated temperatures by soft X-ray photoelectron spectroscopy (XPS) and X-ray diffraction (XRD). The former provided changes in chemical composition and chemical states of elements of the carbon film, and the latter identified crystallites growing in the matrix. The procedures and the devices used are described elsewhere[5, 6, 11].

3. Results and Discussion

The reaction product of a given system was a metallic carbide; namely, Be_2C, Mo_2C and W_2C for C(H)/Be, C(H)/Mo and C(H)/W, respectively. Figure 1 shows the time-course of Be_2C formation for the C(H)/Be sample at different temperatures, where the ordinate shows the extent of reaction and the abscissa is the reaction time. The completion of Me_2C formation is given by the extent of reaction of $x = 1$.

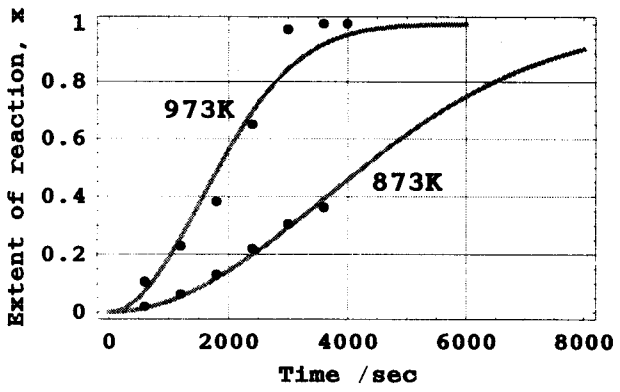

Fig.1. Isothermal reaction curves for C(H)/Be at 873 and 973K

It is seen in the figure that the reaction rate was very small at the beginning, became progressively greater with time in the middle and then decreased to zero at the end of the reaction. This kind of sigmoidal reaction curves is generally explained by nucleation and crystal growth mechanism.

Then the reaction kinetics was analyzed by a random nucleation and subsequent growth model [12, 13]. According to Hulbert[13], the nucleation and crystal growth model gives the extent of a solid-state reaction (x) for n-dimensional growth at time t as

$$-\ln(1-x) = C_n \int_{t'=0}^{t'=t} ID^{n/2}(t-t')^{n/2}\, dt', \tag{1}$$

where C_n is a constant depending on the shape (dimension) of growing crystallites, I the nucleation rate per unit volume and D the diffusion constant of reacting material. The extent of reaction is defined by the ratio of the volume of product crystallites to that of non-reacted reactant matrix, where the product crystallites are grown from product nuclei yielded at time t'. The extent of reaction thus defined has the same meaning determined from compositions measured by XPS as well as XRD.

In the case of one-dimensional growth, a crystallite grows as a needle of radius r. It is a cylinder with thickness of h for two-dimensional growth, and a sphere for three-dimensional case. The shape factors are described as

$$C_1 = \pi r^2, \quad C_2 = \pi h, \quad C_3 = \frac{4\pi}{3} \tag{2}$$

The nucleation can be assumed to obey the first order kinetics[13]. Then, the number of nucleation sites remaining at time t is given by

$$N_t = N_0 \exp(-f\,t), \tag{3}$$

where N_0 is the initial number of nucleation sites per unit volume, f the nucleation frequency per site. Accordingly, the nucleation rate per unit volume is expressed as

$$I = f\,N_t = fN_0 \exp(-f\,t) \tag{4}$$

Substitution of Eq.(4) into Eq.(1) and the integration result in

$$-\ln(1-x) = (\frac{2C_n}{n+2})D^{n/2} f N_0 \exp(-f\,t)\, t^{(n+2)/2} \tag{5}$$

Figure 2 shows SEM photographs of a carbon film after vacuum heating at 1273 K for 10 minutes. The film had been deposited on a tungsten substrate. Many dark spots were observed and their sizes were around 10 μm in diameter. These spots were not observed for the as-deposited film. After prolonged heating, this sample gave XRD peaks corresponding to W_2C. Namely, it appears that those spots are growing W_2C crystallites. In addition, the crystallites are not needle-like and then the growing mode should be two- or three-dimensional. On account that the carbon film was thin in comparison with the radius of growing crystallites, the growth mode is expected to be in two-dimensional.

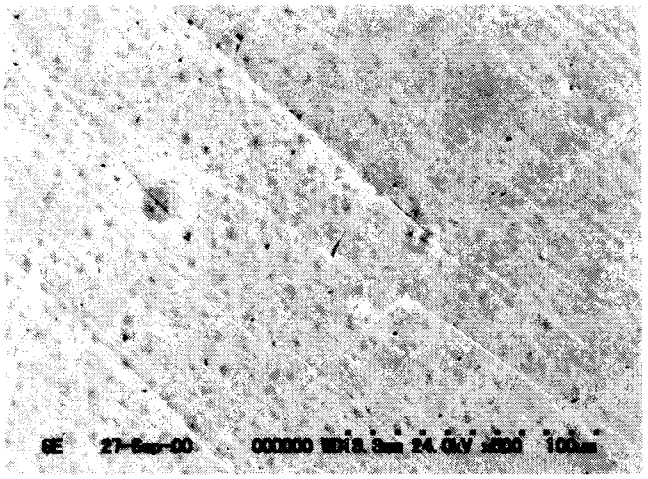

Fig.2. SEM photograph of the evaporated carbon film on W after vacuum heating at 1273 K for 10 min. (× 500)

Accordingly it was assumed that the carbide crystallites grow in a two-dimensional mode for C(H)/Be, C(H)/Mo and C(H)/W. Then the following kinetic equation

$$-\ln(1-x) = (\frac{1}{2})\pi h D f N_0 \exp(-ft)\, t^2 \quad \text{(two-dimensional)} \tag{6}$$

was applied for analyses. The isothermal reaction curves for C(H)/Be were analyzed by Eq.6 with a non-linear fitting method, by which f and D could be evaluated by assuming the number of nucleation sites and the thickness of the carbon film on Be. The former was assumed to be as $N_0 = 1 \times 10^{23}/\mathrm{cm}^3$. The thickness was taken as $h = 0.5 \times 10^{-4}$cm, which was the average thickness of the film measured by SEM observations.

The non-linear fit gave the values as $f = 1.86 \times 10^{-13}$/sec and $D = 2.62 \times 10^{-14}$ cm^2/sec at 873 K, and $f = 4.27 \times 10^{-13}$/sec and $D = 6.15 \times 10^{-14}$ cm^2/sec at 973 K. The solid lines in Fig.1 are calculated reaction curves using these values. The calculated curves agree fairly well with the observations. This implies that the reaction kinetics can be explained well with the nucleation and the two-dimensional growth model.

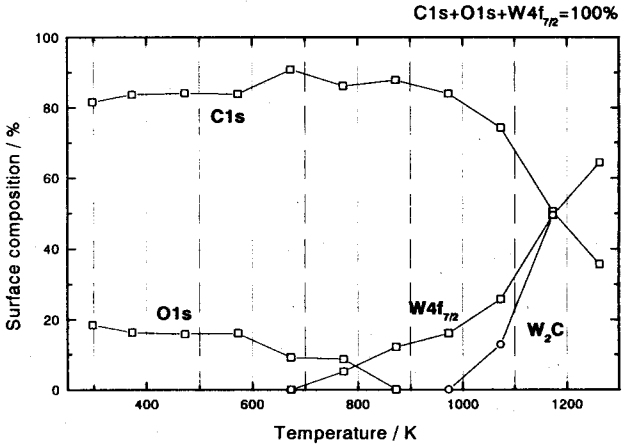

Fig.3. Non-isothermal reaction curves for C(H)/W observed by XPS

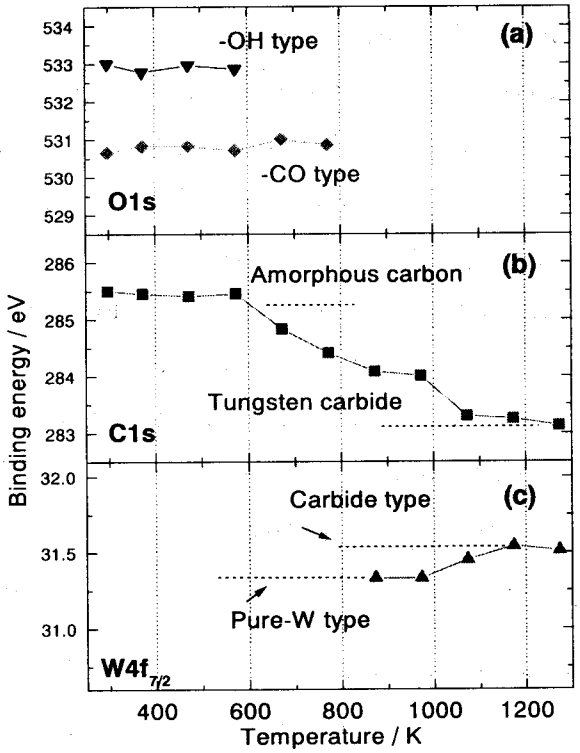

Fig.4. Changes in chemical shifts of XPS peaks for C(H)/W with temperature

Figure 3 shows the change in surface composition with heating, where the surface composition was determined from the areas of C1s, O1s and W4f$_{7/2}$ peaks observed by XPS. It should be mentioned here that the same sample was measured step by step by heating up to 1273 K in a 100 K interval. Namely, a sample was first heated to a given temperature for 10 minutes and then XPS measurements were carried out after cooling down the sample to room temperature. Subsequently the sample was heated further at a higher temperature for 10 minutes and then XPS spectra were measured at room temperature. The procedures were repeated up to 1273 K. It is seen in the figure that the as-prepared sample was covered with carbon deposited and oxygen. The presence of oxygen was ascribed to adsorbed -OH and -CO, depending on the sample preparation conditions and the

exposure to air for transferring the sample from the sample preparation system to the XPS device. The details have been described elsewhere[6, 7]. Tungsten appeared at 773 K and its composition increased with temperature, attaining to 64 at% at 1273 K. On the contrary, the carbon composition started to decrease at 973 K, reaching to 36 at% at 1273 K.

Figure 4 shows the chemical shifts of O1s, C1s and $W4f_{7/2}$ peaks with heating. It is seen in the figure that the as-deposited carbon was amorphous and gradually changed to the carbide type with elevating temperature. Tungsten appeared at first metallic and gradually changed to a carbide type. According to the chemical composition and the shift, the resultant carbide could be identified as W_2C. The formation of W_2C has been also confirmed by X-ray analysis. The chemical shift of $W4f_{7/2}$ peak suggests that the carbide type tungsten was null below 973 K, whereas almost all tungsten was in the carbide state above 1173 K. In the middle, around 1073 K, about one half of the tungsten appeared was metallic and the other in the carbide state. On account of this observation, the growth of W_2C could be shown as the open circles in Fig. 3, which is considered to be a kind of reaction curve, although it was taken under the non-isothermal conditions.

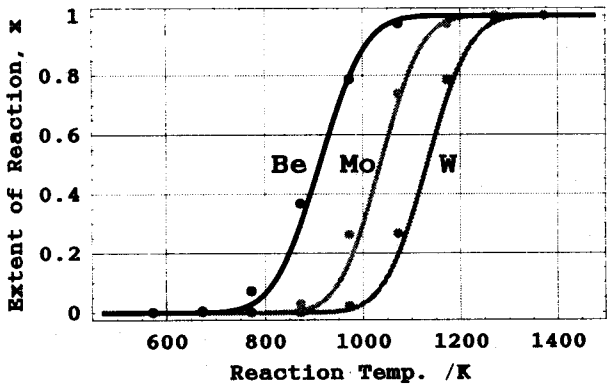

Fig.5. Non-isothermal reaction curves for C(H)/Be, C(H)/Mo and C(H)/W

Figure 5 shows this kind of reaction curves of carbide formation for C(H)/Be, C(H)/Mo and C(H)/W measured with XPS [4, 5, 6, 7], where the ordinate is the reaction extent, x, which was obtained by normalization of the metal composition to the composition of respective carbide, Me_2C. These reaction curves cannot be analyzed by use of Eq.(6). But it was found above that the random nucleation frequency, f, is very small for C(H)/Be and then the exponential term in Eq.(6) is essentially unity under the experimental conditions. Therefore, Eq.(6) can be approximated as

$$-\ln(1-x) = k_{app}\, t^2, \tag{7}$$

where $k_{app} = (\frac{1}{2})\pi h D f N_0$. This equation appears to be also valid for C(H)/Mo and C(H)/W. In addition, it contains only one fitting parameter. Therefore, the apparent rate constant could be evaluated from the non-isothermal reaction curves. The solid lines in Fig.5 are calculated reaction curves using the apparent rate constant, k_{app}, evaluated from the data analyses. The calculated curves agreed well with the observations. This means that the hydrogen-containing carbon films react with the substrate metals through the same reaction mechanism, the random

nucleation and two-dimensional crystal growth. The difference in the reactivity can be ascribed to the differences in the nucleation frequency and/or the diffusivity of relevant elements for respective systems.

The analyses of the non-isothermal reaction curves gave the apparent rate constants at different temperatures for the three systems. Figure 6 shows their temperature dependence. The Arrhenius plots resulted in fairly good straight lines, from which the temperature dependences were determined as

$$k_{app}(\mathrm{Be}) = 3.10\exp(-109.[\mathrm{kJ/mol}]/RT) \quad [1/\mathrm{sec}^2] \tag{8}$$

$$k_{app}(\mathrm{Mo}) = 231.\exp(-161.[\mathrm{kJ/mol}]/RT) \tag{9}$$

$$k_{app}(\mathrm{W}) = 516.\exp(-183.[\mathrm{kJ/mol}]/RT) \tag{10}$$

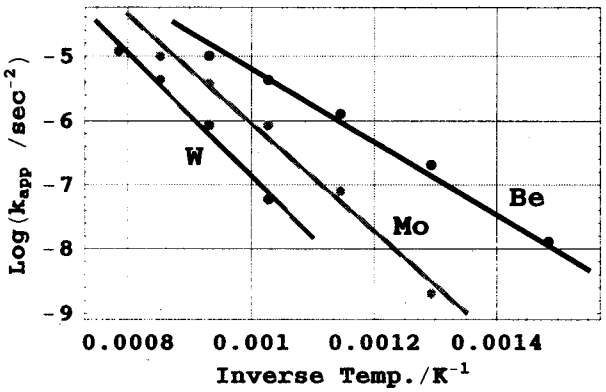

Fig.6. Arrhenius plots of the apparent rate constants for C(H)/Be, C(H)/Mo and C(H)/W

According to Eq.(6), the temperature dependence of the apparent rate constant is expressed as

$$k_{app} = (\frac{1}{2})\pi h N_0 f_0 D_0 \exp[-(\Delta E_f + \Delta E_D)/RT]. \tag{11}$$

It is assumed here that only the nucleation frequency and the diffusion constant have the temperature dependence, where ΔE_f and ΔE_D are the activation energies for nucleation and diffusion, respectively, and f_0 and D_0 are the corresponding frequency factors. Then the apparent activation energy, ΔE_{app}, is the the sum of ΔE_f and ΔE_d.

Although the diffusion constant of carbon in Be is not known, those for Mo and W are reported to be $D_{\mathrm{C/Mo}} = 2.9\times10^{-2}\exp(-172/RT)$ and $D_{\mathrm{C/W}} = 9.2\times10^{-3}\exp(-169/RT)$, where the activation energy and the frequency factor are in the unit of [kJ/mol] and [cm^2/sec], respectively[14]. It should be mentioned, however, that rather widely scattered values of the activation energy for carbon diffusion can be seen in literature. For example, the reported values for tungsten range from 158 to 224

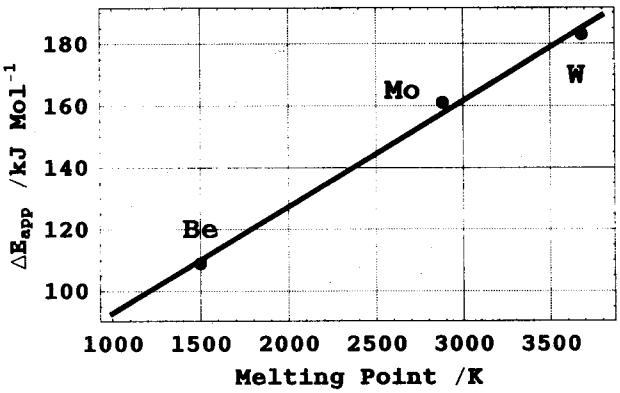

Fig.7. Relation between ΔE_{app} and melting point of substrate

kJ/mol[15]. Nevertheless, it should be noted that the apparent activation energies, E_{app}, appeared in Eqs.(9) and (10) are quite close to the respective activation energies for carbon diffusion. This suggests that the reaction is limited by the diffusion of carbon in the matrix metals, but the nucleation reaction should be almost temperature independent in this case. On the other hand, it is also plausible that the nucleation reaction required a moderate amount of activation energy, and hence the activation energy for diffusion should be lower than those for carbon diffusion in metal matrices. This will take place for carbon diffusion through grain boundaries of reaction products, interfaces between reactant and product, etc.

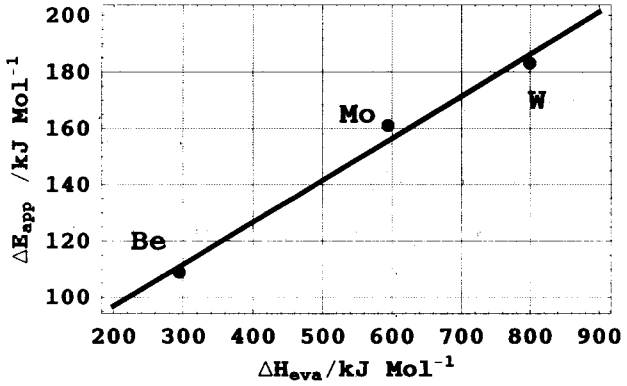

Fig.8. Relation between ΔE_{app} and heat of evaporation of substrate

Good linear relations have been observed between the reactivity of C(H)/Me (Me=Be,Mo,W) and physical properties of the substrate metals, where the reactivity was expediently defined by the temperature required for attaining to the half-way to the completion of Me_2C formation under the given experimental conditions[7]. These relations could be refined by applying the apparent activation energy, ΔE_{app}, as follows. Figure 7 shows a relation between ΔE_{app} and the melting point of substrate metals. It is seen in the figure that the apparent activation energy changes linearly with the melting point of the substrate metal. Essentially the same relation was found for the heat of evaporation of the substrate as seen in Fig.8. These relations indicate that the reaction proceeds more easily on a substrate having smaller binding energy for Me-Me bond.

This relation, however, does not necessarily suggest that the chemical reaction, the nucleation in the present case, plays the predominant role. This is because the Me-Me bond strength has a close correlation to the activation energy for carbon diffusion in respective matrices as seen in Fig.9. In this figure the activation energy for carbon diffusion is plotted against the heat of evaporation of metals constructing BCC and HCP structures, where respective data were cited from literature[14]. There appears a trend that the activation energy for carbon diffusion increases almost linearly with

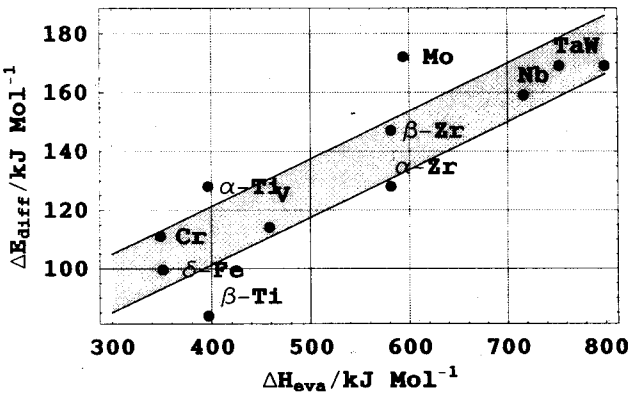

Fig.9. Relation between activation energy for carbon diffusion and heat of evaporation of substrate

the heat of evaporation, namely depending on the strength of Me-Me bond. On account of these relations, it is plausible to conclude that neither of nucleation or diffusion predominates over the others, but they contribute each other to the kinetic process forming Me_2C, as appeared in Eq.(11)

4. Conclusions

Kinetic analyses were carried out for solid-state reactions between a hydrogen-containing carbon film and substrate metals to form metallic carbide of Me_2C (Me = Be, Mo, W). Both of the isothermal and non-isothermal reaction curves could be explained by random nucleation and two dimensional crystal growth model described as

$$-\ln(1-x) = (\frac{1}{2})\pi h D f N_0 \exp(-ft)\, t^2$$

where x is the extent of reaction, f the nucleation frequency per site, h the thickness of film, D the diffusion constant of relevant elements, and N_0 the number of nucleation site per unit volume. The nucleation frequency was found to be very small, and then the equation could be approximated by

$$-\ln(1-x) = k_{app}\, t^2,$$

where $k_{app} = (\frac{1}{2})\pi h D f N_0$. The temperature dependence of the rate constants were evaluated as

$$\begin{aligned} k_{app}(\mathrm{Be}) &= 3.10\exp(-109.[\mathrm{kJ/mol}]/RT) \quad [1/\mathrm{sec}^2], \\ k_{app}(\mathrm{Mo}) &= 231.\exp(-161.[\mathrm{kJ/mol}]/RT), \\ k_{app}(\mathrm{W}) &= 516.\exp(-183.[\mathrm{kJ/mol}]/RT), \end{aligned}$$

for Be-C, Mo-C and W-C systems, respectively, where the apparent activation energy is considered to be the sum of those for nucleation and diffusion. Linear relations were found between the apparent activation energy and the physical properties of substrate metals such as melting point and heat of evaporation.

References

[1] R. Behrisch, A. P. Martinelli, S. Grigull, R. Grotzschel, D. Hildebrandt, and W. Schneider, *J. Nucl. Mater.*, 220-222 (1995) 590

[2] A. Sagara, Y. Hasegawa, and et al, *J. Nucl. Mater.*, 241-243 (1997) 972

[3] V. Philipps and R. Nue, *J. Nucl. Mater.*, 241-243 (1997) 227

[4] K. Ashida, K. Watanabe, N. Ezumi, T. Okabe, and H. Kawamura, *Ann. Rept. HRC. Toyama Univ.*, 15 (1995) 43

[5] K. Ashida and K. Watanabe, *Fusion Engn. Design*, 37 (1997) 307

[6] K. Ashida, K. Watanabe, I. Kitamura, and S. Ikeno, *J. Nucl. Mater.*, 266-269 (1999) 434

[7] K. Ashida, , K. Fujino, T. Okabe, M. Matsuyama, and K. Watanabe, *J. Nucl. Mater.*, 290-293 (2000) 42

[8] K.Ashida and K. Watanabe, *Ann. Rept. Tritium Res. Center, Toyama Univ.*, 6 (1986) 25

[9] 芦田完, 市村憲司, 渡辺国昭, 真　空, 30 (1987) 294

[10] K. Ashida, K. Ichimura, M. Matsuyama, and K. Watanabe, *J. Nucl. Mater.*, 148 (1987) 217

[11] K. Ashida, K. Watanabe, and T. Okabe, *J. Nucl. Mater.*, 241-243 (1997) 1060

[12] J. H. Sharp, G. W. Brindely, and B. N. Narahari Achar, *J. Am. Ceram. Soc.*, 49 (1996) 379

[13] S. F. Hulbert. *J. British Ceram. Soc.*, 6 (1969) 11

[14] 日本金属学会（編）, 金属データブック：改訂２版, Muruzen, Tokyo, Japan, 1984.

[15] W. Eckstein, V. I. Shulga, and J. Roth, *Nucl. Instr. Methods in Phys. Res. B*, 153 (1999) 415